Catalytic Oxidation of NO to NO$_2$ over a H-Mordenite Catalyst*

Jan G. M. Brandin,[†] Lars H. Andersson and C. U. Ingemar Odenbrand

Department of Chemical Technology, Chemical Centre, Lund University, Institute of Science and Technology, P.O. Box 124, S-221 00 Lund, Sweden

A study of the catalytic oxidation of NO to NO$_2$ has been conducted in order to investigate the kinetics of the reaction. The reaction rate dependence of NO partial pressure ($Y_{NO} \leq 600$ ppm, $p_{tot} = 2.1$ bar) was determined to be of first order. A Langmuir–Hinshelwood type dependence was obtained for oxygen, but since the change in oxygen concentration is very small the rate dependence can be regarded as pseudo-zero order. At temperatures above 200 °C the attainable conversion is limited by the thermodynamic equilibrium conversion, and the decomposition of NO$_2$ must be taken into consideration in the model. The apparent pre-exponential factors and activation energies of the rate constants in the resulting model were fitted to experimental data by a least-squares nonlinear regression method. This was done in two different ways, individually to each set of data [mean value of individual fit: $a_1 = 4.3$ mol (g s bar)$^{-1}$, $E_{a1} = 33.4$ kJ mol^{-1}; $a_2 = 4750$ mol (g s bar)$^{-1}$, $E_{a2} = 89.0$ kJ mol^{-1}], and by fitting all data simultaneously [$a_1 = 7.1$ mol (g s bar)$^{-1}$, $E_{a1} = 36.2$ kJ mol^{-1}: $a_2 = 7840$ mol (g s bar)$^{-1}$, $E_{a2} = 91.8$ kJ mol^{-1}].

In order to protect the environment, flue gas denitrification is under introduction in Europe. The technique of selective catalytic reduction of nitrogen oxides with ammonia (SCR) was originally developed in Japan, but in recent years extensive research upon the process has been conducted by european scientists. One important finding is that the rate of reaction is much higher for mixtures of NO and NO$_2$ than for NO alone. The highest rate, about 10 times the NO reduction rate, is obtained for equimolar mixtures. However, since 95 % of the nitrogen oxides in flue gases consist of NO, half this amount must be oxidized to NO$_2$ to take advantage of this finding. In this study we report data on the kinetics of the oxidation of NO with oxygen under conditions prevailing in stack gases over H-mordenite.

In the homogeneous gas-phase oxidation of nitric oxide to nitrogen dioxide, the rate of reaction shows a second-order dependence on nitric oxide partial pressure and a first-order dependence on oxygen partial pressure,[1] eqn. (1). The rate of reaction has the unusual behaviour of

$$r_{NO} = -kp_{NO}^2 p_{O_2} \tag{1}$$

decreasing on an increase in temperature, i.e. the activation energy is negative, −6 to −7 kJ mol^{-1}.

The reason for this is that the reaction proceeds via a dimerized NO complex [(NO)$_2$],[1] reaction (2). Even at
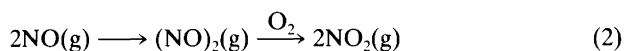
$$2NO(g) \longrightarrow (NO)_2(g) \xrightarrow{O_2} 2NO_2(g) \tag{2}$$

room temperature the degree of dimerization is low, and it decreases at elevated temperatures. By the use of sorbents with a large internal surface area, e.g. silica or activated carbon, the rate of reaction can be enhanced by "physical catalysis". The nitric oxide molecules are adsorbed physically on the surface of the sorbent by van der Waals forces. The local concentration of NO will thus be higher at the surface than in the gas bulk. This results in an increased formation of dimers, and consequently in an increased rate of reaction. In contrast to the homogeneous gas-phase oxidation and the oxidation enhanced by "physical catalysis", the catalytic oxidation of nitric oxide is temperature activated, i.e. the rate increases at increased temperatures. To
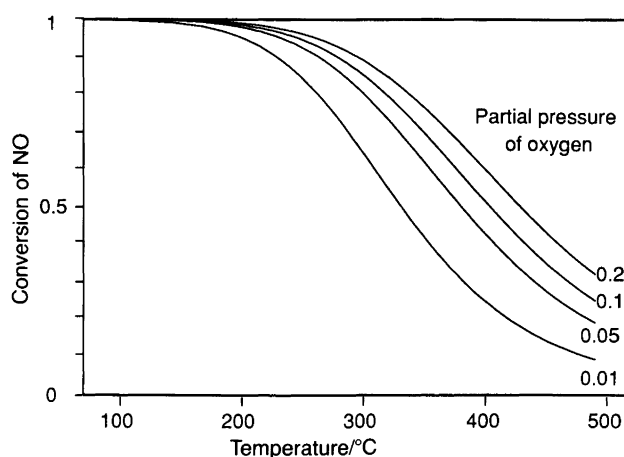

Fig. 1. Equilibrium conversion in the oxidation of NO to NO$_2$ at various partial pressures of oxygen. Total pressure 1 atm.

---

obtain activities of commercial interest, the oxidation must be performed at higher temperatures (150–400 °C, space velocity 10^4–10^5 h^{-1}), e.g. on an aluminosilicate like mordenite. The conversion in this temperature range will be limited by the thermodynamic equilibrium (Fig. 1).

Experimental

Apparatus and analysis. The catalytic reactor, the analytic system and the catalyst used have been described before, but a brief description is given below.[2-4] The reactant gases were supplied from gas cylinders with known concentrations of the components and dosed by the aid of mass-flow regulators. Sample streams for analysis were taken before and after passage of the catalytic bed while maintaining a constant flow through the reactor. The contents of NO and NO_2 were determined by chemiluminescence. The concentration of O_2 was calculated from the calibrated mass flow regulators. The catalyst bed with catalyst amounts of 0.2–3.5 g could be operated in both integral and close to differential modes. The inside diameter of the stainless-steel tubular reactor was 5 mm and the particle size was 0.3 mm. The effect of diffusion limitations was evaluated using measured reaction rates and physiochemical characteristics of the catalyst as described before.[5] The only gradients present were the internal gradients for concentrations of NO and NO_2. Effectiveness factors were in the range of 0.5. The kinetics determined was thus only slightly influenced by diffusion processes.

The catalyst. The catalyst used in this study is a mordenite called Zeolon 900H from Norton Co. It has been characterized previously and some of the characteristics are summarized below.[2-4] The Si/Al molar ratio is 5.34 and the contents of metallic ions are: Fe 0.50, Ti 0.26, Na 0.18, K 0.15 and Ca 0.09 wt% of the hydrated catalyst. All metallic ions are present in exchange positions except for Ti, which is present as a TiO_2 impurity. The surface area is 472 m^2 g^{-1} and the pore volume for pore radii from 2 μm to 1000 Å, measured by Hg-porosimetry, is 0.13 cm^3 g^{-1}. The pore volume for pore radii below 1000 Å, measured by the BET method, is 0.207 cm^3 g^{-1}, of which the major part (0.180 cm^3 g^{-1}) is contained in micropores with diameters below 16 Å. The adsorption of NO was studied by IR spectroscopy and the presence of NO$^+$ was eastablished. The amount of NO$^+$ was shown to be correlated with the amount of aluminium atoms in the structure. Activities in the oxidation of NO to NO_2 were reported previously and could be correlated with the amount of aluminium in acid leached mordenites.[2]
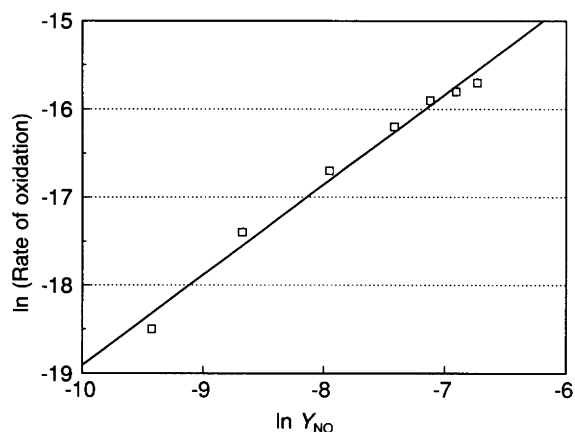
Results

Determination of the reaction orders. The reaction orders for NO and O_2 were evaluated under differential conditions at 250 °C. In one series the molar fraction of NO in the inlet was varied from 50 to 600 ppm while the oxygen molar

Table 1. Results from the variation of the NO molar fraction. Temperature = 250 °C, Y_{O_2} = 0.021, G_{TOT} = 60 Nl h^{-1}, gas load = 109 Nl (h g)$^{-1}$, p_{tot} = 2.1 bar.

Molar fraction of NO /ppm	Measured rate×10^{-7} /mol (g s)$^{-1}$	Measured conversion /%
568	1.53	18.5
477	1.40	19.8
384	1.20	20.8
286	0.91	20.9
168	0.54	21.3
81	0.27	22.0
38	0.09	16.7

fraction was kept constant at 2.0 %. In another series the molar fraction of NO was kept at 600 ppm, while the oxygen molar fraction was varied from 3000 ppm to 4 %. The total gas flow was 60 Nl h^{-1} (Nl is l at STP) and the gas load was 109 Nl (g h)$^{-1}$. The result obtained is given in Table 1. By plotting the natural logarithm of the measured rate versus the natural logarithm of the average molar fraction of NO, the reaction order for nitric oxide was determined from the slope to be about 1 (Fig. 2). Obviously the rate of reaction is directly proportional to the partial pressure of NO at these low values of the partial

Fig. 2. Determination of the reaction order for NO at 250 °C, G_{TOT} = 60 Nl h^{-1}, gas load = 109 Nl (g h)$^{-1}$, Y_{O_2} = 0.02, p_{tot} = 2.1 bar. Slope = 1.02.

Table 2. Results from the variation of the O_2 molar fraction. Temperature = 250 °C, Y_{NO}= 600 ppm, G_{TOT} = 60 Nl h^{-1}, gas load = 109 Nl (h g)$^{-1}$, p_{tot} = 2.1 bar.

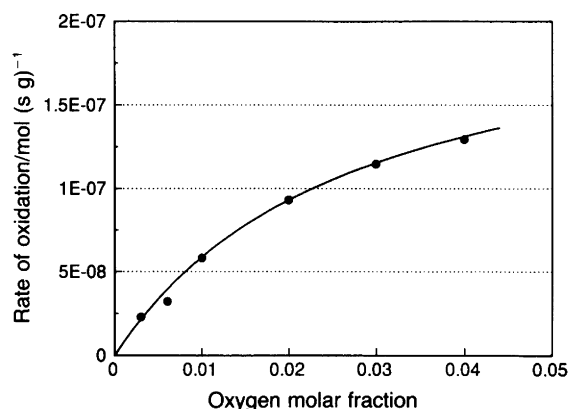| Molar fraction of O_2	Measured rate×10^{-7} /mol (g s)$^{-1}$	Measured conversion /%
0.003	0.23	2.9
0.006	0.32	4.1
0.010	0.58	7.3
0.020	0.93	11.8
0.030	1.15	14.7
0.040	1.30	16.7

Fig. 3. The rate of oxidation as a function of oxygen molar fraction, at 250 °C, G_{TOT} = 60 Nl h^{-1}, Gas load = 109 Nl (g h)$^{-1}$, Y_{NO} = 600 ppm, p_{tot} = 2.1 bar.

pressure. The same approach applied to the oxygen dependence resulted in a reaction order of 0.7. This low value suggests a mechanism of the Langmuir–Hinshelwood type. The result obtained is given in Table 2. By plotting p_{O_2}/r_a against p_{O_2}, it is possible to determine the constants of eqn. (3), where Y_{NO} and Y_{O_2} are the molar fraction of NO

$$r_a = -\frac{k_1 K_{O_2} Y_{NO} Y_{O_2} p_{tot}^2}{1 + K_{O_2} Y_{O_2} p_{tot}} \text{ mol (g s)}^{-1} \tag{3}$$

$$k_1 = 1.77 \times 10^{-4} \text{ mol (bar g s)}^{-1}$$

$$K_{O_2} = 17.14 \text{ bar}^{-1}$$

and O_2, respectively, and p_{tot} the total pressure in bar. The result of the model fitting is shown in Fig. 3.

Determination of the apparent rate constants in the reversible temperature range. Under integral conditions, the conversion was measured as a function of temperature using varying amounts of catalyst (3.5, 2.0, 1.2, 0.4 and 0.2 g). The other conditions were kept constant at F_{NO} = 4.3×10^{-7} mol s^{-1}, p_{tot} = 2.1 bar, Y_{NO} = 600 ppm and a total flow of 60 Nl h^{-1}.

When the integral conversion is approaching the equilibrium conversion at higher temperatures, it is necessary to take the reverse reaction into account, i.e. the decomposition of NO_2 into NO.

Since the experimental adsorption order for oxygen was one, we concluded that the adsorption for oxygen must be molecular. The following reactions and assumptions lead to the rate expression (9) with a first-order dependence on nitrogen dioxide.

(i) Molecular adsorption of oxygen on a vacancy (V):

$$O_2(g) + V \underset{k_2}{\overset{k_1}{\rightleftharpoons}} O_2(ads) \tag{4}$$

$$K_{O_2} = k_1/k_2$$

(ii) Reaction from the gas phase of NO with the adsorbed O_2 forming an adsorbed O and gaseous NO_2:

$$NO(g) + O_2(ads) \underset{k_4}{\overset{k_3}{\rightleftharpoons}} O(ads) + NO_2(g) \tag{5}$$
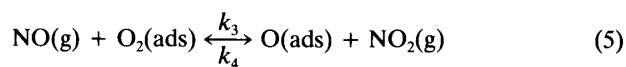
(iii) Rearranging the adsorbed O forming adsorbed O_2 and vacancies:

$$2O(ads) \underset{k_6}{\overset{k_5}{\rightleftharpoons}} O_2(ads) + V \tag{6}$$

$$K_{56} = k_5/k_6$$

If the reaction of NO with adsorbed O_2, reaction (5), is chosen as the rate-limiting step, the rate equation (7) can be derived, in which S_{TOT} is the total number of sites [eqn. (8)]. If this model would describe the actual process, it

$$r_{OX} = \frac{-k_3 K_{O_2} S_{TOT} p_{NO} p_{O_2} + k_4 (K_{O_2}/K_{56})^{1/2} S_{TOT} p_{NO_2} p_{O_2}^{1/2}}{1 + (K_{O_2}/K_{56})^{1/2} p_{O_2}^{1/2} + K_{O_2} p_{O_2}} \tag{7}$$

$$S_{TOT} = [V] + [O_2(ads)] + [O(ads)] \tag{8}$$

must be assumed that $(K_{O_2}/K_{56})^{1/2}(p_{O_2})^{1/2} \ll K_{O_2} p_{O_2}$ in the numerator of the rate equation. With this assumption, the derived oxygen dependence is in accordance with the observed oxygen dependence. Since the change in oxygen partial pressure is very small, both the rate of oxidation and the rate of the reverse reaction will be of pseudo-zero order in oxygen partial pressure. These assumptions result in the rate expression given by eqn. (9) in which k_1' and k_2' are given by eqns. (10) and (11), respectively. At equilibrium

$$r_{NO} = -k_1' p_{NO} + k_2' p_{NO_2} \tag{9}$$

$$k_1' = \frac{k_3 K_{O_2} p_{O_2} S_{TOT}}{1 + K_{O_2} p_{O_2}} \tag{10}$$

$$k_2' = \frac{k(K_{O_2}/K_{56})^{1/2} p_{O_2}^{1/2} S_{TOT}}{1 + K_{O_2} p_{O_2}} \tag{11}$$

the forward and reverse reaction rates are equal [eqn. (12)] and the equilibrium equation is given by eqn. (13). By the use of eqns. (12) and (13), k_2' was eliminated to give eqn. (14). The rate expression was integrated from the differ-

$$k_1'(p_{NO})_{eq} = k_2'(p_{NO_2})_{eq} \tag{12}$$

$$\frac{p_{NO_2(eq)}}{p_{NO(eq)} p_{O_2}^{1/2}} = K_p \tag{13}$$

$$k_2' = \frac{k_1'}{K_p p_{O_2}^{1/2}} \tag{14}$$

Table 3. Results from the nonlinear least-squares regression fit to each amount of catalyst.

Amount /g	a_1 /mol $(s\ g\ bar)^{-1}$	E_{a1app} /kJ mol^{-1}	$a_2{}^a$ /mol $(s\ g\ bar)^{-1}$	$E_{a2app}{}^a$ /kJ mol^{-1}
0.2	3.89	30.3	4293	85.8
0.4	2.45	30.3	2708	85.8
1.2	2.86	31.8	3116	87.4
2.0	6.01	34.6	6624	90.4
3.5	6.42	36.6	6713	92.2

^{a}Calculated from $k'_2 = k'_1/K_p (p_{O_2})^{1/2}$.
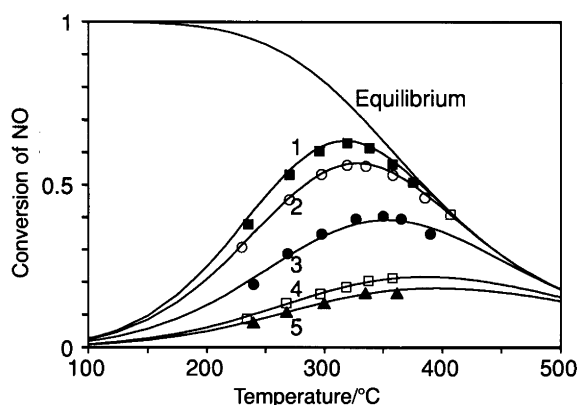

Fig. 4. Simulation of the kinetics for the oxidation of NO with O_2. Individual fit of the model to each amount of catalyst. Experimental conversion versus temperature at different amounts of catalyst: (1) 3.5, (2) 2.0, (3) 1.2, (4) 0.4, (5) 0.2 g. Lines represent simulated data. Y_{NO} = 600 ppm, Y_{O_2} = 0.021, G_{TOT} = 60 Nl h^{-1}, p_{tot} = 2.1 bar.

ential material balance for the fixed bed reactor, and the conversion was isolated [eqns. (15) and (16)]. The equilib-

$$X = X_{eq}(1 - e^{-K})$$ (15)

$$K = p_{O_2}p_{NO} \frac{W}{F_{NO}} k'_1 \left(1 + \frac{1}{K_p p_{O_2}^{1/2}}\right)$$ (16)

rium constant was calculated from eqn. (17). The values of enthalpy and entropy was calculated from NASA polynoms[6] and the value given by eqn. (18) was obtained. The equilibrium conversion was calculated from eqn. (19).

$$\ln K_p(T) = -\frac{\Delta H(T)}{RT} + \frac{\Delta S(T)}{R}$$ (17)

$$K_p = 1.8777 \times 10^{-4} \exp(55.55\ kJ\ mol^{-1}/RT)\ (bar^{-1/2})$$ (18)

$$X_{eq} = \frac{K_p p_{O_2}}{(1 + K_p p_{O_2}^{1/2})}$$ (19)

The parameters of the model, E_{a1} and a_1, were fitted to the measured conversion by a nonlinear least-squares re-

gression method. The rate constant k'_2, and indirectly the parameters E_{a2} and a_2, were calculated from expression (14) above. The results from the fit are given in Table 3 and Fig. 4. The values of the activation energies in Table 3 seem to vary with the amount of catalyst. This is probably a combined effect of the scattering in the result and the uncertainty of freely optimizing two independent constants in an equation. The rate constant should be independent of the amount of catalyst. As shown in Fig. 5 the data are independent of the amount of catalyst, except for the lowest value (0.2 g).

From the mean value of the rate constant at each temperature average values of the pre-exponential factor and the activation energy were calculated. The values obtained are given in Table 4. In a second approach a fit to the whole data set was conducted. The results from the fit are given in Table 4 and Fig. 6.
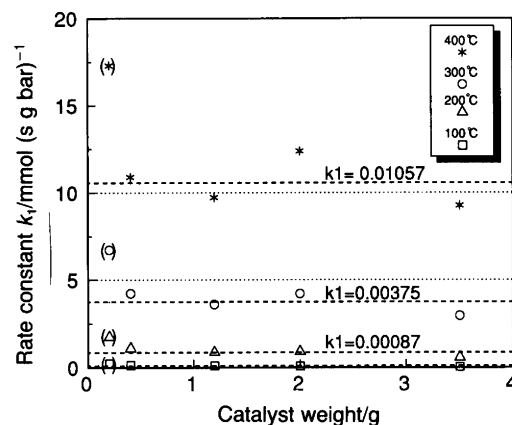

Fig. 5. Calculated value of the rate constant k'_1, from the individual fit to each amount of catalyst, versus the amount of catalyst at different temperatures.
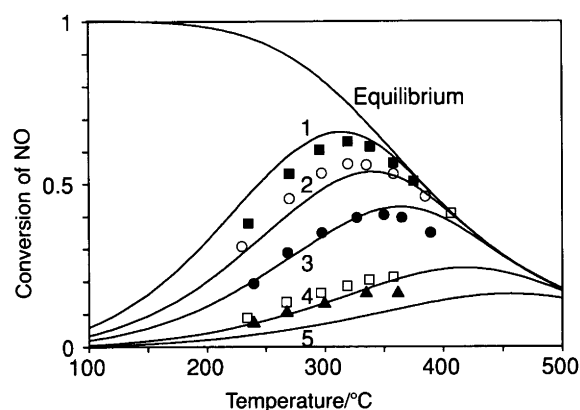

Fig. 6. Simulation of the kinetics for the oxidation of NO with O_2. Simultaneous fit to all data. Experimental conversion versus temperature at different amounts of catalyst: (1) 3.5, (2) 2.0, (3) 1.2, (4) 0.4, (5) 0.2 g. Lines represent simulated data. Y_{NO} = 600 ppm, Y_{O_2} = 0.021, G_{TOT} = 60 Nl h^{-1}, p_{tot} = 2.1 bar.

Table 4. Pre-exponential factor (a_1) and apparent activation energy (E_{a1app}) from the individual fit and from the fit to all data.

Type of fit	a_1 /mol (s g bar)$^{-1}$	σ	E_{a1app} /kJ mol^{-1}	σ	a_2 /mol (s g bar)$^{-1}$	E_{a2app} /kJ mol^{-1}
Mean value of individual fit	4.31	1.62	33.4	1.21	4750	89.0
Fit to all data	7.1	2.67	36.2	1.77	7840	91.8

Summary

A study of the catalytic oxidation of NO to NO_2 over an H-mordenite catalyst has been performed in order to investigate the kinetics of the reaction. The reaction orders for NO and O_2 were determined under differential conditions at 250 °C. The rate dependence on nitric oxide was found to be of first order at these low partial pressures ($Y_{NO} \leq 600$ ppm, $p_{tot} = 2.1$ bar). The dependence on oxygen was shown to be of the Langmuir–Hinshelwood type, but since the change in concentration was very small, it could be regarded as pseudo-zero order. At high temperatures the attainable conversion is limited by the thermodynamic equilibrium conversion. This was taken into consideration by introducing the reverse reaction, namely the decomposition of NO_2 into NO and O_2. The model was fitted in two different ways, an individual fit for each amount of catalyst, and a fit to the whole data set simultaneously. Excellent agreement between the model and the experimental data is obtained if each amount of catalyst is fitted individually. When the whole data set is used simultaneously a fairly good agreement is obtained.

List of symbols

p_{tot}	Total pressure (bar)
p_{NO}, p_{O_2}	Partial pressure (bar)
Y_{NO}, Y_{O_2}	Molar fraction of NO and O_2
r_{NO}	Rate of reaction in the oxidation of NO to NO_2 [mol (g s)$^{-1}$]
k_1-k_6	Rate constants
K_{O_2}	Adsorption constant of O_2, $K_{O_2} = k_1/k_2$ (bar^{-1})
K_{56}	Equilibrium constant in eqn. (6), $K_{56} = k_5/k_6$
V	oxygen vacancy
O_2(ads)	Molecular adsorbed oxygen
O(ads)	Atomic adsorbed oxygen
k'_1	Apparent rate constant in the oxidation of NO to NO_2 [mol (g s bar)$^{-1}$]
k'_2	Apparent rate constant in the decomposition of NO_2 to NO [mol (g s bar)$^{-1}$]
a_1, a_2	Apparent pre-exponential factors for k'_1 and k'_2 [mol (g s bar)$^{-1}$]
E_{a1}, E_{a2}	Apparent activation energies for k'_1 and k'_2 (kJ/mol)
K_p	Equilibrium constant in the oxidation of NO to NO_2 (bar$^{-1/2}$)
X, X_{eq}	Conversion of NO and equilibrium conversion of NO
W	Amount of catalyst (g)
F_{NO}	Molar flow of NO (mol s^{-1})
G_{TOT}	Total volume flow (Nl h^{-1})
Nl	l at STP
S_{TOT}	Total number of sites

References

1. Scholten, J. J. F. and Zwietering, P. Actes Int. Congr. Catalyse, 2^e, Technip, Paris 1960, Vol. 1, p. 389.
2. Odenbrand, C. U. I., Andersson, L. A. H., Brandin, J. G. M. and Järås, S. Catal. Today 4 (1989) 155.
3. Andersson, L. A. H., Odenbrand, C. U. I. and Brandin, J. G. M. Catal. Today 4 (1989) 173.
4. Brandin, J. G. M., Odenbrand, C. U. I. and Andersson, L. A. H. Catal. Today 4 (1989) 187.
5. Odenbrand, C. U. I., Lundin, S. T. and Andersson, L. A. H. Appl. Catal. 18 (1985) 335.
6. Gardiner, W. C., Jr. Combustion Chemistry, Springer-Verlag, New York 1984, p. 485.